European Journal of Pharmaceutical Sciences 65 (2014) 147–155

Contents lists available at ScienceDirect

European Journal of Pharmaceutical Sciences

journal homepage: www.elsevier.com/locate/ejps

# *In vitro* metabolism, disposition, preclinical pharmacokinetics and prediction of human pharmacokinetics of DNDI-VL-2098, a potential oral treatment for Visceral Leishmaniasis

Rao Mukkavilli [a], Jakir Pinjari [a], Bhavesh Patel [a], Shankar Sengottuvelan [a], Subodh Mondal [a], Ajit Gadekar [a], Manas Verma [a], Jignesh Patel [a], Lavanya Pothuri [a], Gopu Chandrashekar [a], Prabhakar Koiram [a], Tanukrishnan Harisudhan [a], Ansari Moinuddin [a], Delphine Launay [b], Nimish Vachharajani [a], Vikram Ramanathan [a], Denis Martin [b,*]

[a] *Advinus Therapeutics Ltd., Bangalore, India*
[b] *Drugs for Neglected Diseases Initiative, Geneva, Switzerland*

ARTICLE INFO

*Article history:*
Received 15 April 2014
Received in revised form 8 August 2014
Accepted 5 September 2014
Available online 27 September 2014

*Keywords:*
Allometric scaling
Bioavailability
Bioanalysis
Cytochrome P450
Preclinical pharmacokinetics

ABSTRACT

The *in vitro* metabolism and *in vivo* pharmacokinetic (PK) properties of DNDI-VL-2098, a potential oral agent for Visceral Leishmaniasis (VL) were studied and used to predict its human pharmacokinetics. DNDI-VL-2098 showed a low solubility (10 μM) and was highly permeable (>200 nm/s) in the Caco-2 model. It was stable *in vitro* in liver microsomes and hepatocytes and no metabolite was detectable in circulating plasma from dosed animals suggesting very slow, if any, metabolism of the compound. DNDI-VL-2098 was moderate to highly bound to plasma proteins across the species tested (94–98%). DNDI-VL-2098 showed satisfactory PK properties in mouse, hamster, rat and dog with a low blood clearance (<15% of hepatic blood flow except hamster), a volume of distribution of about 3 times total body water, acceptable half-life (1–6 h across the species) and good oral bioavailability (37–100%). Allometric scaling of the preclinical PK data to human gave a blood half-life of approximately 20 h suggesting that the compound could be a once-a-day drug. Based on the above assumptions, the minimum efficacious dose predicted for a 50 kg human was 150 mg and 300 mg, using efficacy results in the mouse and hamster, respectively.



## 1. Introduction

Visceral Leishmaniasis (VL) is a tropical disease caused by protozoan parasites of the genus Leishmania and it is transmitted by the bite of certain species of the sand fly. Also called *Kala Azar*, the disease is endemic in parts of north-eastern India, sub-Saharan Africa, parts of the Mediterranean, and South America. The disease has world-wide distribution in Asia, East Africa, South America and the Mediterranean regions. It kills 200,000–300,000 people a year in the Indian subcontinent alone and is also greatly debilitating to those who survive the infection.

Currently, pentavalent antimonials, amphotericin B administered through IV route, and paramomycin administered through IM route are the only first-line treatments for VL. Resistance to antimonials has reached 60% in Bihar state in India (Sundar et al., 2000, 2012) whereas amphotericin is expensive to procure and must be given as an IV infusion in a clinical setting. Paramomycin

*Abbreviations:* AUC, area under the concentration–time curve; BCRP, breast cancer resistant protein; BID, twice a day dosing; Caco-2, human epithelial colorectal adenocarcinoma cells; $C_b$, concentration in blood; $C_p$, concentration in plasma; CC, calibration curve; CYP, cytochrome P-450; CL, *in vivo* clearance; $CL_{intr}$, intrinsic clearance; CPCSEA, committee for the purpose of control and supervision of experiments on animals; DNDi, Drugs for Neglected Diseases *initiative*; F, oral bioavailability; $F_b$, fraction bound to plasma proteins; HBSS, Hank's Balanced Salt Solution; HEPES, 4-(2-hydroxyethyl)-1-piperazineethanesulfonic acid; HPLC, high performance liquid chromatography; $IC_{50}$, concentration causing 50% inhibition; IV, intravenous; IM, intramuscular; LC/MS/MS, liquid chromatography tandem mass spectrometry; n, number of replicates; LLE, liquid–liquid extraction; MTBE, methyl tertiary butyl ether; NADPH, nicotinamide adenine dinucleotide phosphate; PK, pharmacokinetics; Pgp, P-glycoprotein; PO, Per Oral; QC, quality control; QD, once a day dosing; QH, hepatic flow; $t_{1/2}$, half-life; UV, ultraviolet; VL, Visceral Leishmaniasis; $V_{ss}$, volume of distribution at steady state.

* Corresponding author at: Drugs for Neglected Diseases Initiative, 15 chemin Louis Dunant, 1202, Geneva, Switzerland. Tel.: +41 22 906 92 30.
*E-mail address:* dmartin@dndi.org (D. Martin).

http://dx.doi.org/10.1016/j.ejps.2014.09.006
0928-0987/

is administered as intramuscular injection. Miltefosine is being used as an oral treatment in India, Columbia, Brazil, and Germany but major concerns exist over patient safety, compliance and sub-optimal use leading to development of resistance (Olliaro et al., 2005; Romero and Boelaert, 2010; Van Griensven et al., 2010). There is thus an urgent need for a new oral and cost-effective treatment.

The Leishmania parasite resides predominantly in the liver and spleen. Oral administration has a particular advantage for VL as blood from the intestine containing orally absorbed drug first reaches the liver, the site of the parasite, prior to entry into the general circulation.

DNDI-VL-2098 was recently identified as a potent anti-leishmanial compound as a result of an effort by the Drugs for Neglected Diseases *initiative* (DND*i*) to screen compounds originally synthesized as antitubercular agents by the TB Alliance. The compound is a nitro-imidazo-oxazole and the (R)-enantiomer (Fig. 1) was selected for advanced evaluation. Other nitro-heterocyclic compounds (*e.g.* 5- and 2- nitroimidazoles and 5-nitrofurans) are effective against various protozoan and bacterial infections in humans and animals. Although nitro groups in compounds are sometimes associated with mutagenic characteristics, DNDI-VL-2098 has been shown to be non-mutagenic in the Ames test.

DNDI-VL-2098 was potent *in vitro* in a macrophage amastigote model against several strains including the standard *Leishmania donovani* strain, an Indian antimony resistant strain (DD8, $IC_{50}$ = 0.025 μM), and against recently isolated clinical strains from Africa ($IC_{50}$ = 0.7–2.6 μM). *In vivo*, in both an acute mouse model of the disease (50 mg/kg for 5 days; greater than 99% parasite inhibition) and in a chronic hamster model, DNDI-VL-2098 showed greater than 85% parasite inhibition. In this latter model DNDI-VL-2098 consistently showed greater efficacy and longer duration of effect than the racemate and the (S)-enantiomer (Gupta et al., 2013). This greater efficacy in a stringent animal model of leishmaniasis justified the choice of (R)-enantiomer for advanced evaluation.

Studies using a chiral bioanalytical assay showed that *in vitro* in microsomes and hepatocytes, and *in vivo* in blood following dosing, (R)-DNDI-VL-2098 does not undergo chiral interconversion to the (S)-enantiomer.

As part of the preclinical evaluation an extensive characterization of the *in vitro* and *in vivo* preclinical pharmacokinetic properties of (R)-DNDI-VL-2098 was performed.

## 2. Methods

### 2.1. Chemicals

DNDI-VL-2098 was synthesized at Advinus Therapeutics Limited, Bangalore, India. The Caco-2 cell line (human colon carcinoma epithelial cell line) was obtained from ATCC (HTB-37, Manassas, USA) and cells were used at passage number 40. Corning Transwell® filters 12-well, HBSS, HEPES, glucose and sodium bicarbonate were obtained from Sigma Aldrich (Bangalore, India). Liver microsomes, hepatocytes, hepatocyte isolation kits, Waymouth's media were purchased from Xenotech LLC (Kansas, USA). Purified recombinant CYP450 isozymes, CYP1A2, CYP2C9, CYP2C19, CYP2D6 and CYP3A4 were purchased from BD Biosciences (Woburn, USA). For the blood to plasma concentration ratio study, freshly collected mouse, rat and dog blood was obtained from in-house animals. Human blood was obtained from the Blood Bank (Bangalore, India). For the protein binding study, a 96-well equilibrium dialyser with 150 μL half-cell capacity (HTDialysis®, Gales Ferry, USA) employing 12–14,000 Dalton molecular weight cut-off membranes was used. Standard substrates, metabolites, inhibitors, NADPH and deuterated analytical internal standards used for the CYP inhibition study were obtained from Sigma–Aldrich (Bangalore, India), BD Biosciences (Woburn, USA) and TRC (Toronto, Canada).

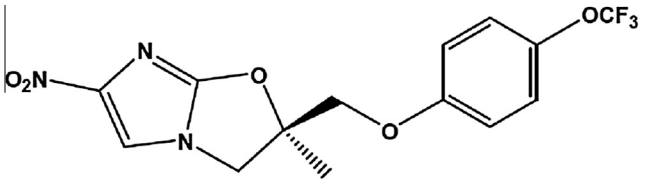


**Fig. 1.** Structure of DNDI-VL-2098.

### 2.2. Animal husbandry and handling

All animal studies had the approval of the Institutional Animal Ethics Committee of Advinus Therapeutics Ltd. (an Association for Assessment and Accreditation of Laboratory Animal Care accredited facility) and were in accordance with the guidelines of the Committee for the Purpose of Control and Supervision of Experiments on Animals (Government of India). Animals were acclimatized in study rooms for at least three days prior to dosing. Hamsters and mice were housed in polypropylene cages (3 per cage, marked for identification), rats were housed singly and dogs were housed in individual pens maintained in controlled environmental conditions (22 ± 3 °C; 40–70% Relative Humidity; 10–15 fresh air change cycles/h) with 12 h light and dark cycles. All animals were bred in-house except hamsters which were obtained from the Central Drugs Research Institute, Lucknow, India. Hamsters, mouse and rats were given Ssniff® Rodent pellet food (ssniff Spezialdiäten GmbH, Germany) *ad libitum* and dogs were given Pedigree® standard dog chow (manufactured by Effem India Private Limited, India) 300 g once a day. Good quality water passed through activated charcoal filter and exposed to UV rays was provided *ad libitum* throughout the study to all animals.

In hamsters and mice, blood samples were collected through retro-orbital plexus using a sparse sampling design. In rats and dogs, a serial sampling design was used with blood samples withdrawn through jugular vein in rats and cephalic vein in dogs. In rats, surgery was performed 48 h before study conduct and no surgery was performed in dogs.

### 2.3. In vivo pharmacokinetic studies

#### 2.3.1. Formulations

The IV solution vehicle comprised 20% (v/v) N-methyl-2-pyrrolidinone (NMP) and 40% (v/v) polyethylene glycol 400 (PEG-400) in 100 mM citrate buffer pH 3. The PO vehicle comprised 7% (v/v) Tween® 80 and 3% (v/v) ethanol in water for hamster and mouse studies. Oral solutions in rat and dog used the same vehicle as IV. Suspension formulations comprised 0.08% (v/v) Tween® 80 in 0.5% (w/v) sodium carboxymethyl cellulose (medium viscosity). The IV dose volume was 1 mL/kg for hamsters, rats and dog and 2 mL/kg for mice. The oral dose volume was 10 mL/kg for hamsters and mice, 5–10 mL/kg for rats and 2–5 mL/kg for dogs. Formulations were prepared on the day of dosing.

#### 2.3.2. Surgery in rats

Rats were anesthetized using 1 mL/kg body weight of a mixture of ketamine (40 mg/mL) and xylazine (4 mg/mL). The depth of anesthesia was assessed by sensory and motor responses. Rats were placed in supine position and a 2 cm ventral cervical skin incision was made on the right side. Tissues were cleaned to visualize jugular vein following which a sterile PE-50 cannula was inserted into the vein and secured in place with a suture. The cannula was exteriorized through the scapulae. Skin incisions were sutured, sodium heparin (5000 IU/mL) was flushed through the

cannula and stoppered using stainless steel pin. Every day patency was assessed to ensure no blocking of cannula.

*2.3.3. Dosing*

For IV bolus dose administration, hamsters and mice were dosed through the tail vein, rats through the jugular vein and dogs through the saphenous vein. The oral dose was administered by gavage for all animals.

*2.3.4. PK studies*

Studies were performed in healthy male golden Syrian hamsters (30 g), Swiss Albino mice (30–40 g), Sprague Dawley rats (250–300 g) and Beagle dogs (10–13 kg). Hamsters and mice were fasted 4 h prior to dosing and food was provided 4 h post dose. Rats and dogs were fasted overnight and were provided food 4 h post dose. A sparse sampling design was used in hamsters and mice ($n = 3$ per time point). Serial blood sampling was used for rat (parallel groups; $n = 4$) and dog (crossover; $n = 3$). In hamster, approximately, 100 μL blood samples was collected ($K_2$EDTA anticoagulant, 20 μL/mL, 200 mM) at 0.083 (only IV), 0.25, 0.5, 1, 2, 4, 6, 12 and 24 h post-dose. In mouse and rat, blood samples were collected at 0.083 (only IV), 0.25, 0.5, 1, 2, 4, 6, 8, 10, 24, 48, and 72 h (only rat, not mouse) post-dose. In the dog, blood samples were collected at 0.083 (only IV), 0.25, 0.5, 1, 2, 4, 8, 10, 24, 48, and 72 h post-dose. Studies in dog using corn oil suspension, samples were collected at 0, 0.25, 0.5, 1, 2, 3, 6, 12, 24, 48, 72 and 120 h following single oral dose administration (QD); following BID dosing (dose administration at 0 and 8 h), samples were collected at 0, 0.25, 0.5, 1, 1.5, 2, 3, 6, 8, 8.25, 8.50, 9.00, 9.5, 10, 11, 14, 16, 24, 48, 72, 96 and 120 h. In each case a 75 μL aliquot of blood was mixed with 75 μL of 0.1 M HCl, vortex-mixed and centrifuged (2600*g*, 5 min), and the supernatant was stored below −60 °C until analysis.

*2.3.5. Pharmacokinetic analysis*

Pharmacokinetic parameters were calculated using non-compartmental analysis tool of validated WinNonlin® software (Version 5.2). The area under the concentration time curve ($AUC_{last}$ and $AUC_{inf}$) was calculated by linear trapezoidal rule. The peak concentration ($C_{max}$) and time for the peak concentration ($T_{max}$) were the observed values. The elimination rate constant value ($k_{el}$) was obtained by linear regression of the log-linear terminal phase of the concentration–time profile using at least 3 non-zero declining concentrations in terminal phase with a correlation coefficient of >0.8. The terminal half-life value ($t_{1/2}$) was calculated using the equation $0.693/k_{el}$. Allometric methods were used to predict human blood clearance, volume of distribution and half-life (Chaturvedi et al., 2001; Mehmood and Balian, 1996; Sharma and McNeill, 2009).

*2.4. In vitro studies*

*2.4.1. Solubility of DNDI-VL-2098 by UV spectrometry*

Solubility of DNDI-VL-2098 was assessed up to 100 μM by spiking dimethylsulfoxide (DMSO) stock solutions (10 μL, duplicate) into 990 μL buffer in a 96-well plate and placing at room temperature for 2 h. Calibration standards were prepared by spiking 5 μL of DMSO stock solutions into 995 μL acetonitrile:buffer (1:1) mixture. Following centrifugation (1700*g*, 20 min, 25 °C) the supernatant was diluted 1:1 with acetonitrile and analyzed using a Tecan M200 UV spectrophotometer.

*2.4.2. Caco-2 permeability*

Permeability of DNDI-VL-2098 (10 μM) was determined in apical to basolateral (A–B) and basolateral to apical (B–A) directions. Transport studies were conducted 21 days post seeding in 12-well Transwell® inserts. Following pre-incubation in HBSS-HEPES buffer in an orbital shaker (37 °C, 5% $CO_2$, 30 min), trans-epithelial electric resistance (TEER) values were measured and only those inserts with values above 300 Ω $cm^2$ were considered for assay. HBSS-HEPES buffer was removed and DNDI-VL-2098 spiked HBSS-HEPES buffer (1% final DMSO concentration) was added to each donor compartment in triplicate. Blank HBSS-HEPES buffer containing 1% DMSO was added to the receiver compartment. Samples were withdrawn from the receiver chamber at 30, 60, 90, and 120 min, and from the donor chamber at 0 and 120 min. TEER values were measured after completion of assay to ensure monolayer integrity. At the end of the experiment, cells were washed with cold buffer and lysed with acetonitrile to assess cell accumulation and estimate the recovery. Apparent permeability ($P_{app}$), efflux ratio ($P_{app(B-A)}/P_{app(A-B)}$), cell accumulation (concentration in buffer and acetonitrile wash) and recovery (total amount recovered/initial amount added) were calculated. Rhodamine-123 (substrate for P-gp) was run as positive control.

*2.4.3. Microsomal stability*

Microsomes from males of golden Syrian hamster, CD-1 mouse, Sprague–Dawley rat, and Beagle dog, and mixed gender human (pool of 50) were used for assays. Incubations (1 mL) consisted of liver microsomes (0.5 mg/mL), NADPH (2 mM) and 50 mM phosphate buffer (pH 7.4). Following pre-incubation (10 min, 37 °C), reactions were initiated by adding DNDI-VL-2098 (0.5 μM). Samples (50 μL) were withdrawn at 0, 3, 6, 9, 12, 15, 18, 21, 27 and 30 min and quenched with 50 μL acetonitrile containing internal standard. Concomitant NADPH-free control incubations were made similarly with samples collected at 0 and 30 min. Verapamil (hamster, mouse and dog liver microsomes) and diclofenac (rat and human liver microsomes) were concomitantly used as positive control substrates.

*2.4.4. Stability in hepatocytes*

Hepatocyte suspensions (CD-1 mouse, Wistar rat, Beagle dog, human; male) containing $10^6$ cells/mL were used for the incubations. Following pre-incubation of cell suspension (995 μL, 10 min, 37 °C, 5% $CO_2$), reactions were initiated by addition of 5 μL DNDI-VL-2098 stock solution (final concentration in assay was 0.5 μM). Samples (100 μL) were taken at 0, 5, 15, 30, 60, and 90 min, and quenched with 100 μL acetonitrile. Hepatocyte-free control incubations were prepared by spiking 5 μL of DNDI-VL-2098 into 995 μL of Waymouth's media, and aliquots (100 μL) were taken at 0 and 90 min. A cocktail mixture containing phenacetin, diclofenac, 7-hydroxycoumain, bufuralol and midazolam was concomitantly used as positive control substrates.

*2.4.5. CYP phenotyping*

Incubations (1 mL) consisted of purified isozyme (50 pmol and 100 pmol, CYP1A2, 2C9, 2C19, 2D6 and 3A4), NADPH (2 mM) and 50 mM phosphate buffer (pH 7.4). After pre-incubation (10 min, 37 °C), reactions were initiated by adding DNDI-VL-2098 (0.5 μM). Samples (100 μL) were taken at 0, 10, 20, 30, 40, 50, and 60 min and quenched with 100 μL acetonitrile. NADPH-free incubations were made similarly with samples at 0, 30 and 60 min. 7-ethoxyresorufin, diclofenac, omeprazole, dextromethorphan and midazolam were concomitantly used as positive control substrates for CYP1A2, 2C9, 2C19, 2D6 and 3A4, respectively.

*2.4.6. Blood to plasma concentration ratio*

Fresh blood (1 mL) was spiked with DNDI-VL-2098 to produce 0.3, 3, 30 μg/mL (0.08% DMSO). After gentle inversion, for the $t_0$ time point, a 50 μL aliquot was hemolyzed by adding 50 μL 1% formic acid and snap-frozen. A second 200 μL aliquot was taken to generate plasma, 50 μL of which was mixed with 50 μL 1% formic acid and snap-frozen. The remaining blood sample was incubated

at 37 °C and blood and plasma samples were similarly taken at 30 and 60 min.

*2.4.7. Plasma protein binding*

Plasma was spiked with DNDI-VL-2098 to produce 0.3, 3, 30 μg/mL (0.08% DMSO). After gentle inversion, six replicates of 50 μL each were collected at $t_0$ to determine spiking accuracy, and another 500 μL sample was incubated in a microfuge tube (4 h, 37 °C, 5% $CO_2$) to assess stability. Binding was determined by adding 120 μL of DNDI-VL-2098 spiked plasma to one half-cell (donor, $n = 6$) of equilibrium dialyser and 120 μL buffer to the receiver compartment. The assembled dialyzer was incubated (37 °C, 5% $CO_2$, 120 rpm) for 4 h, after which plasma and buffer samples were recovered from each half-cell and samples were analyzed. Diclofenac was concomitantly used as a positive control compound.

*2.4.8. CYP inhibition*

Buffer, CYP substrates and microsomes (0.15 mg/mL except 0.25 mg/mL for CYP2C19 and 0.10 mg/mL for CYP3A-midazolam) were mixed and aliquots were transferred into a 96-well plate. CYP isozyme-specific probe substrates used were CYP1A2 (phenacetin, 45 μM), CYP2C9 (Diclofenac, 10 μM), CYP2C19 (S-mephenytoin, 55 μM), CYP2D6 (dextromethorphan, 10 μM), and CYP3A (midazolam, 5 μM). DNDI-VL-2098 stock solutions were spiked (1 μL) to achieve the final target inhibitor concentrations (0.012, 0.024, 0.049, 0.098, 0.195, 0.39, 0.78, 1.56, 3.125, 6.25, and 12.5 μM). Following pre-incubation (5 min, 37 °C), reactions were initiated by adding 20 μL of 20 mM NADPH and the plate was incubated at 37 °C. At preset time points (5 min for CYP3A-midazolam, 7 min for CYP2C9 & CYP2D6, 10 min for CYP1A2, and 40 min for CYP2C19), the reactions were quenched with acetonitrile, or 1% formic acid:acetonitrile 70:30 for CYP1A2. All experiments were run in triplicate ($n = 3$). Deuterated metabolite internal standards were added and *in situ* production of the corresponding CYP isozyme-specific metabolite (CYP1A2-acetaminophen, CYP2C9-4-hydroxydiclofenac, CYP2C19-4-hydroxymephenytoin, CYP2D6-dextrorphan, CYP3A-1-hydroxymidazolam) was determined. α-napthoflavone, sulfaphenazole, benzylnirvanol, quinidine and ketoconazole were concomitantly run as positive control inhibitors for CYPs 1A2, 2C9, 2C19, 2D6 and 3A4, respectively. The concentration of test inhibitor required for 50% reduction in the measured isozyme activity ($IC_{50}$) was estimated using GrapPad Prism® software.

*2.4.9. Samples for routes of biotransformation*

Samples for *in vitro* biotransformation were obtained following incubation of DNDI-VL-2098 (10 μM) with microsomes in presence of cofactors, and with hepatocytes for up to 120 min as described for metabolic stability. Samples for *in vivo* biotransformation were oral PK blood samples at 4, 6 and 8 h post dose from mouse (50 mg/kg), rat (500 mg/kg) and dog (50 mg/kg). All samples were precipitated with acetonitrile, vortex-mixed and centrifuged (1700*g*, 10 min) and the supernatants were analyzed for Phase I and Phase II metabolites.

*2.5. Bioanalysis*

All *in vivo* and *in vitro* samples were analyzed for DNDI-VL-2098 and internal standard (DNDI-VL-2075, a structural analog) content using a high performance liquid chromatography (HPLC, Shimadzu Prominence, Japan) tandem mass spectrometric (API4000, Applied Biosystems, USA) method. Positive-ion electron spray ionization mode was used and MRM transitions of 360.20/175.00 for DNDI-VL-2098 and 370.20/241.20 for DNDI-VL-2075 (5 μg/mL) were monitored. An isocratic HPLC method with a 4 min run time was employed for analysis. The mobile phase comprised 5 mM ammonium formate and acetonitrile 20:80 (v/v) with 0.05% formic acid and the flow rate was 0.6 mL/min. Separation was achieved using Kromasil® C8 column (4.6 × 50 mm, 5 μ, Chromatographie Service, USA) maintained at 40 °C employing an injection volume of 10 μL for *in vivo* samples and 5 μL for *in vitro* samples.

*2.5.1. In vivo samples*

In preliminary studies, DNDI-VL-2098 showed some instability in plasma from different species. Acidification of blood samples from dosed animals with an equal volume of 0.1 M HCl resolved the issue, as bench-top stability of greater than 5 h was achieved; therefore all concentrations were determined in blood. Blood samples were extracted using liquid–liquid extraction (LLE) with methyl tert-butyl ether (MTBE). A 50 μL aliquot of blood, internal standard (20 μL) and potassium dihydrogen phosphate buffer (100 mM, 50 μL) and 1.25 mL of MTBE were vortex mixed and then centrifuged at 2500*g* for 5 min. A 1 mL aliquot of supernatant was evaporated under flow of nitrogen gas at 50 °C until dryness, and the residue was reconstituted with 200 μL of mobile phase before analysis.

The lower limit of quantification (LLOQ) was 5 ng/mL and the assay was linear over a 1000-fold concentration range. All samples were processed along with calibration curve and quality control samples. An acceptance criterion of ±15% was used for all calibration curve (CC), and quality control (QC) standards except for LLOQ sample where ±20% was the acceptance criteria.

*2.5.2. In vitro samples*

Samples were processed by protein precipitation with acetonitrile for all assays except the blood to plasma concentration ratio assay where LLE using MTBE was employed. Processed samples were analyzed for peak area ratios. Samples from studies of protein binding were quantitated using a calibration curve. CC, QC and study samples were prepared using a mixed matrix approach by mixing 5 μL of DMSO (blank/CC/QC), 5 μL of plasma (blank/stability/donor samples) and 50 μL of buffer (blank/receiver samples) followed by protein precipitation using acetonitrile containing internal standard.

Studies using a chiral bioanalytical assay showed that *in vitro* in microsomes and hepatocytes, and *in vivo* in pharmacokinetic plasma samples, (R)-DNDI-VL-2098 does not undergo chiral interconversion to the (S) enantiomer (Bioanalytical manuscript under preparation).

*2.5.3. Routes of biotransformation*

All samples were scanned using a PDA detector (SPD-M20A), LC/MS and LC/MS/MS using positive ($MH^+$), negative ($MH^-$) (Q1) and product ion (MS/MS) scan. A full scan analysis was performed from $m/z$ 100 to $m/z$ 1000. Possible metabolite peaks were identified in positive Q1 scan after assessing for matrix interference using test item free control samples and subsequently confirmed using the fragmentation pattern (MS/MS scan). Samples were run using Kromasil C18 column (150 × 4.6 mm, 5 μ, Chromatographie Service, USA) maintained at 40 °C, employing a linear gradient comprising 0.1% formic acid in water and 0.1% formic acid in acetonitrile, with a 30 min run time. An injection volume of 20 μL was used with a flow rate of 400 μL/min. The concentration of organic phase was fixed at 5% for the initial 6 min, linearly increased to 95% over the next 15 min, held at 95% for the next 9 min, brought back to 5% over the next 2 min followed by equilibration for the next 4 min. The declustering potential was 60 V, entrance potential was 10 V, collision energy for MS/MS was 23 eV, collision gas was 6 Psi, curtain gas was 20 Psi, ion gas 1 was 40 Psi, ion gas 2 was 50 Psi, ion spray voltage was 5500 V and temperature was 500 °C.

## 3. Results

### 3.1. In vivo pharmacokinetics and blood partitioning

The pharmacokinetics of DNDI-VL-2098 was determined in blood as it was found to be unstable in plasma (bench top stability: 30% remaining over 3 h). The mean blood to plasma concentration ratio ($C_b/C_p$) value ranged from 0.55 (human) to 1.24 (mouse) and was similar across the concentration ranges tested (0.3–30 μg/mL, Table 1). These data indicate that DNDI-VL-2098 does not partition extensively into RBCs.

The concentration time profiles for DNDI-VL-2098 are shown in Fig. 2. The compound was well distributed with a steady-state volume of distribution that was 3 times total body water (0.7 L/kg) in the hamster, mouse and rat, and about 4 times total body water in the dog. It showed a low intravenous blood clearance *in vivo* in mouse, rat and dog, and a moderate clearance in the hamster. When expressed as a percentage of the normal hepatic blood flow ($Q_H$), the blood clearance was about 40% in the hamster, 10% in the mouse, 14% in the rat and 17% in the dog (Davies and Morris, 1993). The low *in vivo* clearance of DNDI-VL-2098 is consistent with its high metabolic stability *in vitro* in liver microsomes and hepatocytes, and its generally high oral bioavailability. The oral bioavailability of DNDI-VL-2098 was good to excellent in all four species (Table 2).

### 3.2. Pharmacokinetic linearity

DNDI-VL-2098 showed close to dose proportional exposures in rodents (Table 2). Oral exposure in hamster and mouse were determined across the 6.25–50 mg/kg range (doses tested for efficacy) using formulations identical to those used in efficacy studies. In both species, bioavailability was 100% at the lowest 6.25 mg/kg dose, and in both species an 8-fold increase in dose (from 6.25 to 50 mg/kg) led to an 11-fold increase in exposure. In rat, oral exposures were determined across the 5–500 mg/kg dose range (doses tested in early safety studies) using a suspension in CMC. Here, a 100-fold increase in dose led to about a 100-fold increase in exposure. Fig. 3a summarizes the relationship between dose and dose-normalized AUCs (DNAUC) in various species following suspension administration. The dose-normalized AUCs of DNDI-VL-2098 were generally independent (within 2-fold) of the administered doses.

In the rat and dog, oral solution and suspension exposures were determined at 5 mg/kg. In both species, the mean solution exposure was higher than that with suspension (Fig. 3b). In the dog at the higher dose of 50 mg/kg given as suspension, exposure did not increase proportionally (Table 2). A similar "apparent solubility limited absorption" did not occur in the rat where exposures increased dose-proportionally up to 500 mg/kg given as suspension. This observation is consistent with DNDI-VL-2098 being a low solubility/high permeability compound, with the high permeability overriding any limitation that low solubility may pose to absorption, at least in the rat.

Because exposures increased proportionally with dose in the rat at high doses, follow up studies were performed in the dog at higher doses using a corn oil formulation. As solubility of DNDI-VL-2098 was less in water, an oil-based formulation using corn oil was evaluated. In this case, a 100-fold increase in dose from 5 mg/kg to 500 mg/kg, led to a 37-fold increase in exposure ($AUC_{last}$). By using a 500 mg/kg BID dosing (dosed 8 h apart; total dose 1000 mg/kg), there was a 50% increase in exposure (360 ± 36 μg h/mL; $n = 3$) compared to that obtained at the 1250 mg/kg QD dose (246 ± 74 μg h/mL; $n = 3$, Fig. 4).

**Table 1**
*In vitro* blood to plasma concentration ratio of DNDI-VL-2098.

| Blood/plasma concentration ratio (60 min)[a] | | | | |
|---|---|---|---|---|
| Concentration (μg/mL) | Mouse[b] | Rat[c] | Dog[d] | Human[e] |
| 0.3 | 1.29 | 0.82 | 0.74 | 0.52 |
| 3 | 1.31 | 0.68 | 0.75 | 0.59 |
| 30 | 1.13 | 1.08 | 0.75 | 0.54 |
| Average | 1.24 | 0.86 | 0.75 | 0.55 |

[a] Mean, $n = 2$; Blood collected from males, pool of at least 3 animals/concentration Anticoagulant: 200 mM $K_2$EDTA, 20 μL per mL of blood.
[b] Swiss Albino mice.
[c] Sprague–Dawley rat.
[d] Beagle dog.
[e] Asian.

### 3.3. Prediction of human PK and human efficacious doses

The preclinical PK parameters were used to perform allometric scaling to predict pharmacokinetics in humans. First, simple allometric scaling of the clearance and volume of distribution data was performed using $Y = aW^b$, where $Y$ is the parameter of interest, and $a$ and $b$ are coefficient and exponent of the allometric equation, respectively, and $W$ is body weight. The clearance exponent calculated with this approach was 0.9. Because it exceeded 0.7, the maximum lifespan potential (MLP (years) = (185.4) ($Br^{0.636}$) ($BW^{-0.225}$)) approach was used (Mahmood, 2007). The MLP method gave estimates of 1.69 mL/min/kg for blood clearance and 2.97 L/kg for volume of distribution for a 50 kg human (Fig. 5). These human clearance and volume estimates gave an estimated blood half-life ($T½ = 0.693 \times V_{ss}/CL$) for DNDI-VL-2098 in humans of approximately 20 h, suggesting that the compound is likely to be a once-a-day drug.

To predict human efficacious doses, the model-independent equation for clearance was used: Dose = AUC∗CL/F, where AUC is the targeted $AUC_{inf}$ at the $ED_{99}$ from the preclinical animal model studies. The following assumptions were made: (1) exposure required for efficacy in human will be similar to that at the $ED_{99}$ in the preclinical efficacy models of mice and hamsters, (2) exposures in healthy mice and hamsters at their $ED_{99}$ doses are similar to those in the disease models, (3) human bioavailability will be about 50%, and (4) the predicted human clearance from allometric scaling is an accurate estimate of *in vivo* clearance. Based on the above assumptions, the minimum efficacious dose predicted for a 50 kg human was 150 mg and 300 mg, based on results for the mouse and hamster, respectively (Table 3).

In addition to allometric scaling, the *in vitro* microsomal intrinsic clearance data of VL-2098 (<0.6 mL/min/g liver in mouse, rat, dog and human) were also used to predict the hepatic clearance ($CL_{hep,in\ vitro}$). The prediction was based on the well-stirred model with an assumed intrinsic clearance of 0.6 mL/min/g liver, and used the measured unbound fraction at the highest tested concentration. These results were compared with the observed clearance $CL_{total}$ *in vivo*. In the mouse, the predicted $CL_{hep,in\ vitro}$ was 1.91 mL/min/kg compared to the observed $CL_{total}$ of 9.37 mL/min/kg (2% and 10% of the hepatic blood flow ($Q_h$), respectively). In the rat, the predicted $CL_{hep,in\ vitro}$ was 1.34 mL/min/kg compared to the observed $CL_{total}$ of 8.18 mL/min/kg, (2% and 15% of $Q_h$, respectively). In the dog, the predicted $CL_{hep,in\ vitro}$ was 0.82 mL/min/kg compared to the observed $CL_{total}$ of 5.18 mL/min/kg (3% and 16% of $Q_h$, respectively). Thus, the predicted hepatic clearance using *in vitro* microsomal data results in an under-prediction of the actual total clearance. This is consistent with the possibility of additional non-Phase-I and/or non-hepatic routes of elimination for DNDI-VL-2098 although such a conclusion will require demonstration in future radiolabeled ADME studies. In human, the predicted hepatic clearance from *in vitro* data was 0.84 mL/min/kg and allometric scaling gave a $CL_{total}$ value of 1.69 mL/min/kg. Taken

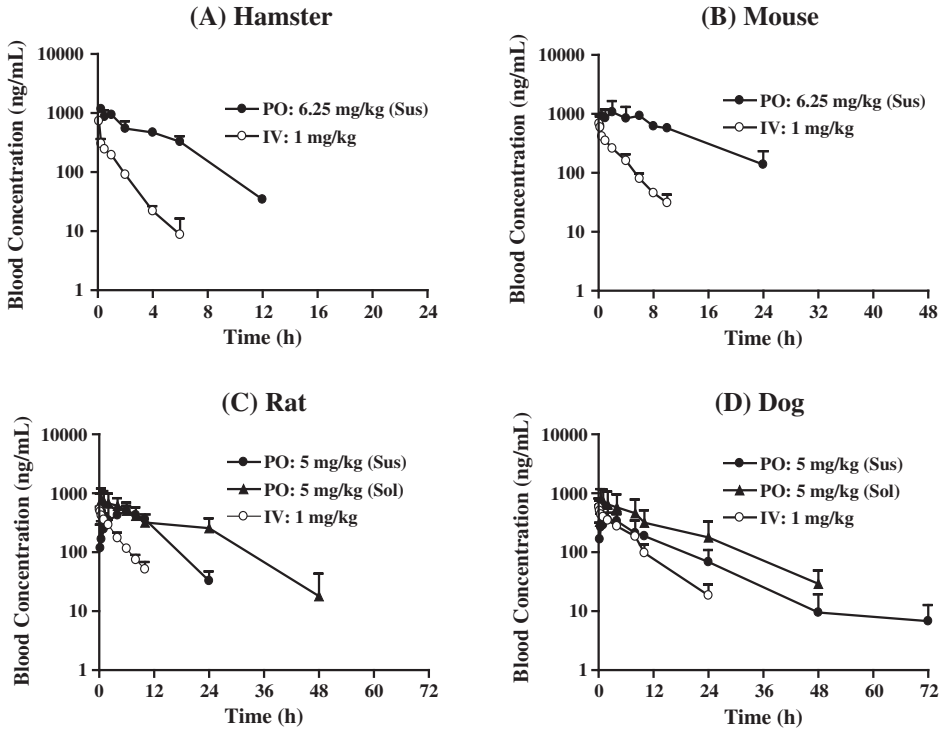


**Fig. 2.** Concentration–time profiles of DNDI-VL-2098 in pharmacokinetic studies in the hamster, mouse, rat and dog.

**Table 2**
*In vivo* pharmacokinetic parameter estimates.

| Species | Dose (mg/kg) | Route | $T_{max}$ (h) | $C_0/C_{max}$ (μg/mL) | $AUC_{last}$ (μg h/mL) | $CL_{blood}$ (mL/min/kg) | $V_{ss,blood}$ (L/kg) | $T_{½}$ (h) | F |
|---|---|---|---|---|---|---|---|---|---|
| Hamster | 1 (Solution) | IV | | 1.14 | 0.63 ± 0.02 | 25.98 | 2.00 | 1.19 | |
| | 6.25 (Suspension) | PO | 0.25 | 1.17 ± 0.99 | 4.49 ± 0.24 | | | | 115 |
| | 12.5 (Suspension) | | 0.50 | 2.36 ± 0.27 | 17.13 ± 0.84 | | | | |
| | 25 (Suspension) | | 4.00 | 3.13 ± 0.16 | 29.80 ± 2.05 | | | | |
| | 50 (Suspension) | | 4.00 | 4.93 ± 0.54 | 53.00 ± 2.82 | | | | |
| Mouse | 1 (Solution) | IV | | 0.74 | 1.65 ± 0.10 | 9.37 | 1.98 | 2.94 | |
| | 6.25 (Suspension) | PO | 2.00 | 1.08 ± 0.33 | 13.10 ± 0.95 | | | | 127 |
| | 12.5 (Suspension) | | 4.00 | 2.43 ± 0.30 | 29.76 ± 1.79 | | | | |
| | 25 (Suspension) | | 4.00 | 5.39 ± 1.12 | 77.23 ± 5.34 | | | | |
| | 50 (Suspension) | | 6.00 | 8.39 ± 0.90 | 145.08 ± 17.30 | | | | |
| Rat | 1 (Solution) | IV | | 0.56 ± 0.09 | 1.84 ± 0.34 | 8.18 ± 1.62 | 2.24 ± 0.53 | 3.44 ± 0.84 | |
| | 5 (Solution) | PO | 1.81 ± 2.79 | 0.86 ± 0.28 | 10.96 ± 2.58 | | | | 119 |
| | 5 (Suspension) | | 4.50 ± 1.91 | 0.57 ± 0.15 | 6.64 ± 1.04 | | | | 72 |
| | 50 (Suspension) | | 5.00 ± 1.15 | 7.13 ± 1.72 | 76.22 ± 8.44 | | | | |
| | 100 (Suspension) | | 6.50 ± 1.00 | 9.99 ± 1.25 | 187.14 ± 91.10 | | | | |
| | 200 (Suspension) | | 7.50 ± 1.91 | 12.75 ± 2.92 | 351.77 ± 68.80 | | | | |
| | 500 (Suspension) | | 12.00 ± 8.16 | 16.90 ± 1.85 | 659.72 ± 176.96 | | | | |
| Dog | 1 (Solution) | IV | | 0.62 ± 0.23 | 3.48 ± 1.86 | 5.18 ± 1.99 | 2.50 ± 1.55 | 6.05 ± 2.85 | |
| | 5 (Solution) | PO | 0.42 ± 0.14 | 0.80 ± 0.37 | 11.28 ± 7.41 | | | | 79 |
| | 5 (Suspension) | | 1.83 ± 1.89 | 0.38 ± 0.12 | 5.53 ± 1.54 | | | | 39 |
| | 50 (Suspension) | | 10.00 ± 12.17 | 0.88 ± 0.51 | 22.79 ± 23.75 | | | | |

Data from sparse sampling profiles for hamster and mouse expressed as mean ± SE using Bailer method; $n = 3$.
Data from serial sampling profiles for rat and dog expressed as mean ± SD; $n = 4$ for rat; $n = 3$ for dog.

together, the half-life estimate using allometric scaling may represent a more conservative estimate than that using the *in vitro* microsomal clearance.

### 3.4. In Vitro metabolism and disposition studies

#### 3.4.1. Solubility and CaCo-2 permeability

DNDI-VL-2098 was soluble up to 10 μM in sodium phosphate buffer (50 mM, pH 7.4) and it was highly permeable across the Caco-2 monolayer ($P_{app}$ greater than 200 nm/s). The efflux ratio was less than 2 indicating that the compound is not a substrate for the efflux transporters Pgp and BCRP (Table 4).

#### 3.4.2. Metabolic stability in vitro in liver microsomes, hepatocytes and purified CYPs

DNDI-VL-2098 generally showed very low intrinsic clearance in liver microsomes and hepatocytes ($CL_{intr}$ < 0.6 mL/min/kg; $n = 3$ in all species except hamster microsomes); these data are consistent

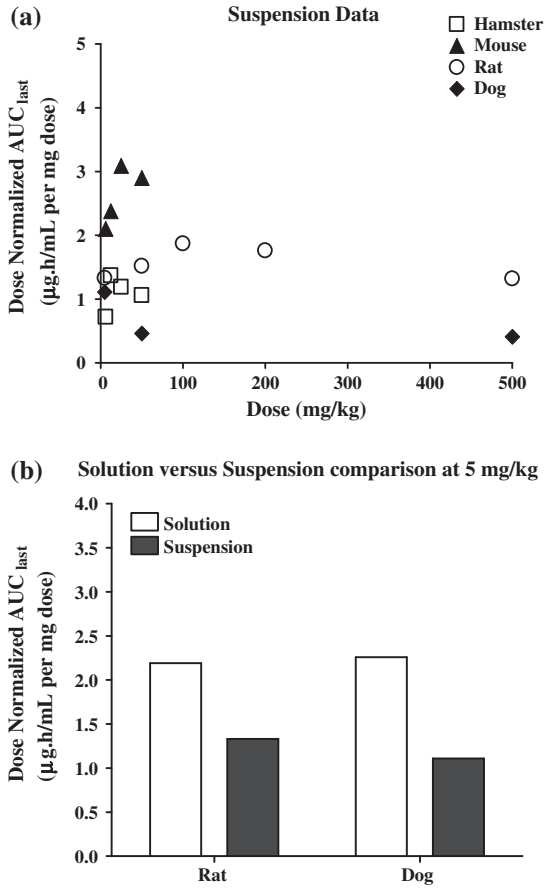


**Fig. 3.** Oral dose-normalized AUC (DNAUC) as a function of administered dose of DNDI-VL-2098 in the hamster, mouse, rat and dog.

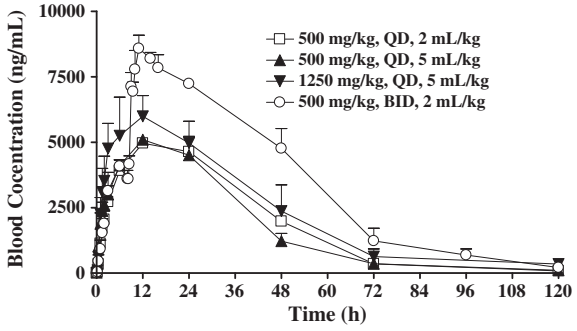


**Fig. 4.** Concentration–time profiles of DNDI-VL-2098 following administration as a corn oil suspension in dogs.

with the low whole body blood clearance in the animal models. In hamster microsomes the $CL_{intr}$ was 2.5 ± 0.2 mL/min/g liver (low to moderate), an observation consistent with its moderate *in vivo* blood clearance (40% of hepatic blood flow) in that species. The $CL_{intr}$ of verapamil and diclofenac exceeded 5 mL/min/g liver, and that of the cocktail of substrates used in hepatocytes matched historical in-house values, indicating that all the preparations were metabolically active.

DNDI-VL-2098 was stable in the tested recombinant human CYPs using 50 pmol and 100 pmol CYP content ($T½ > 60$ min for all isozymes, except CYP2C19 100 pmol where $T½ = 43$ min); this observation is consistent with its high stability in microsomes and hepatocytes. The $t½$ values of concomitantly run positive-controls matched historical in-house values (7-ethoxyresorufin:

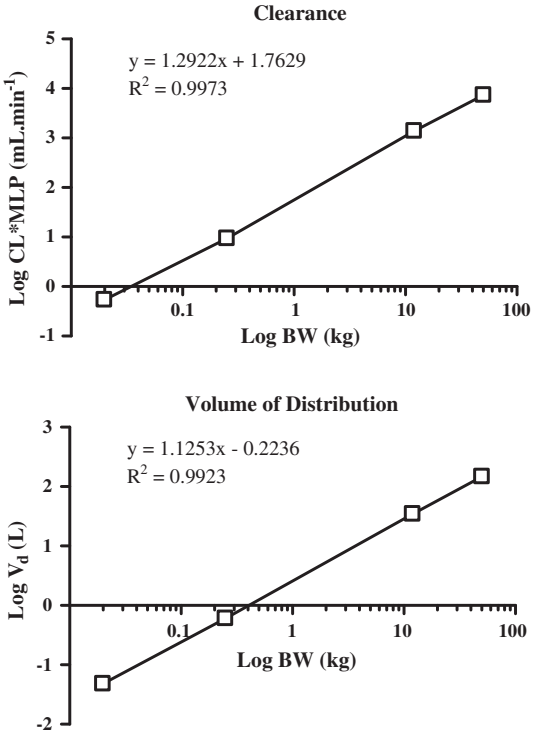


**Fig. 5.** Allometric scaling of blood clearance and steady-state volume of distribution using pharmacokinetic data from preclinical species.

2.3 min, diclofenac: 3.8 min, omeprazole: 2.0 min, dextromethorphan: 0.8 min, testosterone: 11.5 min at 50 pmol CYP content).

### *3.4.3. Protein binding*

DNDI-VL-2098 showed moderate to high binding (Table 5). The unbound fraction was determined to be 3–6% across the species tested. Results for the concomitantly run highly bound compound diclofenac (percentage unbound 0.23 ± 0.10) matched the historical in-house values in this assay.

### *3.4.4. CYP inhibition*

DNDI-VL-2098 did not inhibit CYP1A2, CYP2C9, CYP2D6 and CYP3A4 at concentrations up to 12.5 µM (triplicate $IC_{50}$ studies). It did however inhibit CYP2C19 with an $IC_{50}$ value of 0.47 ± 0.24 µM. $IC_{50}$ values for concomitantly run positive control inhibitors α-napthoflavone, sulfaphenazole, N-3-benzylnirvanol, quinidine and ketoconazole (0.004 µM, 0.32 µM, 0.56 µM, 0.050 µM and 0.011 µM, respectively) matched the historical in-house values in this assay.

### *3.4.5. Biotransformation of DNDI-VL-2098*

A minor monooxygenation metabolite (M-I, 19.44 min) was detected in mouse, rat and dog liver microsomes (<0.2% for mouse, <0.1% for rat and <0.5% for dog assuming similar ionization) based on peak area comparison of metabolite to parent peak, but it was not detected in incubations with human liver microsomes. The likely site of monooxygenation is in the trifluoromethoxyphenyl ring (Fig. 1) based on the fragmentation pattern. The metabolite was not detectable in mouse, rat, dog and human hepatocyte incubations nor in circulating blood samples from mouse (oral 50 mg/kg), rat (oral 500 mg/kg) and dog (oral 50 mg/kg). These results are consistent with studies in liver microsomes and hepatocytes indicating that DNDI-VL-2098 is stable *in vitro*. PA-824, a novel 4-nitroimidazole is currently in phase II clinical trial for tuberculosis (TB) and a structural analog of DNDI-VL-2098, produces 4

**Table 3**
Estimated human efficacious doses.

| Species | $ED_{99}$ (mg/kg) | Efficacious AUC at $ED_{99}$ (ng h/mL) | Predicted human CL (mL/min/kg) | Dose (AUC∗CL/F)[a] (mg/kg) | Dose for 50 kg human (mg) |
|---|---|---|---|---|---|
| Mouse | 6.25 | 14,549 | 1.69 | 2.95 | 148 |
| Hamster | 25 | 30,047 | 1.69 | 6.10 | 305 |

[a] Human bioavailability (F) assumed to be 50%; $ED_{99}$ data was generated at CDRI, Lucknow, India and used as such for predictions.

**Table 4**
Transepithelial transport of DNDI-VL-2098 across CaCo-2 Monolayer.

| Compound | Parameters | A to B | B to A |
|---|---|---|---|
| DNDI-VL-2098 | $P_{app}$ (nm/s) | 226 ± 18 | 247 ± 41 |
| | Efflux ratio | 1.1 | |
| | Intracellular accumulation (%) | 11 ± 0.4 | 18 ± 0.4 |
| | Mass Balance (%) | 95 ± 1 | 105 ± 1 |
| | TEER ($\Omega$ cm$^2$) before and after experiment | >300 | >300 |
| Rhodamine-123 (positive control) | $P_{app}$ (nm/s) | 7 ± 2 | 22 ± 2 |
| | Efflux Ratio | 3 | |
| | Intracellular accumulation (%) | 5 ± 1 | 4 ± 1 |
| | Mass balance (%) | 99 ± 3 | 90 ± 3 |
| | TEER ($\Omega$ cm$^2$) before and after experiment | >300 | >300 |

Mean ± SD, $n$ = 3 per assay.

**Table 5**
Plasma protein binding.

| Plasma protein binding – (% bound)[a] | | | | |
|---|---|---|---|---|
| Concentration (μg/mL) | Mouse[b] | Rat[c] | Dog[d] | Human[e] |
| 0.3 | 96.82 ± 0.27 | 94.62 ± 0.31 | 98.27 ± 0.25 | 97.39 ± 0.59 |
| 3 | 96.68 ± 0.06 | 94.12 ± 0.45 | 94.86 ± 0.31 | 94.26 ± 0.63 |
| 30 | 96.35 ± 0.55 | 94.28 ± 0.60 | 95.60 ± 0.78 | 94.40 ± 0.42 |

[a] Mean ± SD, $n$ = 6; Blood collected from males, pool of at least 3 animals/subjects Anticoagulant: 200 mM $K_2$EDTA, 20 μL per mL of blood.
[b] Swiss Albino mice.
[c] Sprague–Dawley rat.
[d] Beagle dog.
[e] Asian.

metabolites when incubated with human S9 fraction including a major des-nitro metabolite, and seven metabolites with purified Ddn (deazaflavin $F_{420}$ dependent nitroreductase) and mycobacterium tuberculosis (Dogra et al., 2011). No analogous metabolites of DNDI-VL-2098 structurally similar to those of PA-824 were detectable in *in vitro* and *in vivo* samples. In summary, DNDI-VL-2098 is not extensively metabolized in preclinical species *in vitro* and *in vivo*, and in human microsomes and hepatocytes *in vitro*. To understand the disposition and excretion pathways of DNDI-VL-2098, studies with $^{14}$C labeled DNDI-VL-2098 are planned.

## 4. Discussion

DNDI-VL-2098 is a recently identified potent new oral lead compound for Visceral Leishmaniasis that is currently under preclinical development. Convenience of therapy (oral as opposed to parenteral treatment) and patient compliance are important goals for a successful new treatment for VL, particularly because it is endemic in rural areas. As such, DNDI-VL-2098 represents a major breakthrough for an unmet medical need. The studies described here show that DNDI-VL-2098 possesses excellent preclinical *in vitro* and *in vivo* pharmacokinetic properties in a variety of rodent and non-rodent models. Allometric scaling of these data predicts that the compound will have good pharmacokinetics in humans and the predicted efficacious human doses are amenable to development.

The *in vitro* microsomal intrinsic clearance of DNDI-VL-2098, and its *in vivo* clearance in animal models showed a close relationship. *In vitro* intrinsic clearance was very low in microsomes from all species (<0.6 mL/min/g liver), except in the hamster where it was moderately stable (2.5 mL/min/g liver) Rao et al., 2011. Similarly, the *in vivo* blood clearance was low in the mouse, rat and dog, and moderate in the hamster. In all of these cases, even if the blood clearance was assumed to entirely reflect only hepatic clearance, DNDI-VL-2098 would be predicted to have a low hepatic extraction ratio (0.10, 0.14 and 0.17 in mouse, rat and dog, respectively), and a moderate extraction ratio of 0.4 in hamster. These data are consistent with generally good bioavailability of the compound *in vivo*.

The results of the studies suggest that the efficacy of DNDI-VL-2098 seen *in vivo* in animal models (Gupta et al., 2013) results from the potency and pharmacokinetic profile of the parent compound, rather than on any active metabolites. Whether assessed in microsomes, or in hepatocytes, or in blood samples from *in vivo* dosed animals, DNDI-VL-2098 was metabolically stable and there was consistently no evidence for production of any meaningful metabolite based on LC–MS/MS–UV detection. The samples for *in vivo* biotransformation were taken following high oral doses leading to high blood concentration of parent drug. The time points selected for assessment (4–8 h post dose) adequately covered the parent compound half-life (1–6 h). Therefore, inadequate analytical sensitivity or early collection points appears unlikely to affect the ability to detect metabolites. Only one, very minor, monooxygenation metabolite was detectable in liver microsomes from

preclinical species (less than 0.5% of parent; likely mono-oxygenation in the trifluoromethoxyphenyl ring (Rao et al., 2011) but not in those from human. DNDI-VL-2098 was found to be 94–98% bound to plasma proteins, but this extent of protein binding does not limit its efficacy. Taken together, the data suggest that the *in vivo* antiparasitic activity of DNDI-VL-2098 is related to circulating levels of parent drug, and that during further toxicological and clinical development quantification of the parent compound DNDI-VL-2098 will suffice.

The oral absorption properties of DNDI-VL-2098 were generally very good. The compound has a low aqueous solubility (about 10 μM at pH 7.4) and a high permeability (226 nm/s in Caco-2 cells). Its total polar surface area (tPSA) is 91 ($\leqslant$140 Å$^2$) another feature consistent with its good permeability characteristics (Veber et al., 2002). It showed excellent bioavailability at low oral doses in three rodent species (80–100%) consistent with its high permeability and metabolic stability. Moreover, even at high toxicologically relevant oral doses, oral suspension exposure in rats increased linearly with dose over a 100-fold dose range (5 mg/kg to 500 mg/kg) (Harisudhan et al., 2011). Taken together with its low aqueous solubility and high permeability, these data suggest that the high permeability of DNDI-VL-2098 overrides its poor aqueous solubility and enables high oral bioavailability in rodents. In dogs, oral bioavailability appears slightly lower (39–79%) although providing adequate exposure. For a 100-fold increase in dose from 5 mg/kg to 500 mg/kg, a 37-fold increase in exposure was observed. The corn oil formulation was tested as a mean to enhance exposure and QD and BID dosing were assessed. Corn oil is also an accepted vehicle for early toxicity assessment. Following 500 mg/kg BID dosing in corn oil (1000 mg/kg/day), there was a 50% increase in exposure compared to a 1250 mg/kg QD dose. These data indicate that the less than dose-proportional increase in exposure in dogs can be circumvented by using appropriate formulation and dosing frequency for toxicology studies. Importantly, these proof-of-principle data with corn oil in dog suggest that, if needed, other alternative formulation approaches with DNDI-VL-2098 are likely to be similarly successful for human.

Overall the safety impact of any possible drug–drug interactions with DNDI-VL-2098 appears acceptable. DNDI-VL-2098 did not inhibit CYPs 1A2, 2C9, 2D6 and 3A4/3A5 *in vitro* and is unlikely to cause drug–drug interactions mediated by these isozymes. DNDI-VL-2098 did inhibit CYP2C19, for which substrates are comparatively limited as compared to the other major CYPs. They include the proton pump inhibitors lansoprazole and omeprazole; anti-epileptics such as diazepam, phenytoin, and phenobarbitone; the tricyclic antidepressants amitriptyline and clomipramine; and the nitrogen mustard alkylating agent cyclophosphamide. Additionally, the antiplatelet agent clopidogrel and the antimalarial proguanil are converted to their active metabolite by CYP2C19 (Flockhart, 2007). DNDI-VL-2098 itself is very stable *in vitro* in human liver microsomes, hepatocytes and recombinant CYPs suggesting that its own clearance is unlikely to be affected by co-administered drugs. In light of the lack of therapeutic options for Visceral Leishmaniasis, the overall risk-profile for CYP-mediated drug–drug interactions therefore appears acceptable. Further studies are needed to characterize the nature of the CYP2C19 inhibition as well its clinical relevance.

The pharmacokinetic properties of DNDI-VL-2098 in the preclinical species suggest that it has the potential to be a once-a-day drug. Its relatively long half-life *in vivo* in the various animal species ($t½$ = 1.2 h in the hamster, 3 h in mouse, 3.5 h in rat and about 6 h in the dog), result from a combination of a generally low clearance and a moderate volume of distribution across species. Allometric scaling of the preclinical pharmacokinetic data predicts a half-life in humans of about 20 h. The predicted human efficacious dose range of 150–300 mg for DNDI-VL-2098 makes it amenable to further oral solid dosage form design for the upcoming Phase 1 trials in humans.

## 5. Conclusions

DNDI-VL-2098, a lead for treatment of VL with excellent pharmacokinetic properties was identified and developed. DNDI-VL-2098 was assessed in pre-clinical species like mouse and hamster (species for efficacy models), and rat and dog (species for toxicology). In general, DNDI-VL-2098 showed (A) low blood clearance (<15% of hepatic blood flow), (B) low volume of distribution (3 times total body water), (C) acceptable half-life and (D) good oral bioavailability and with acceptable dose linearity. The predicted human efficacious doses are in the 150–300 mg range, making it amenable to oral solid dosage form drug for upcoming Phase I trials in human.

## Acknowledgements

The authors would like to dedicate this paper to the abiding memory of a dear friend, colleague and mentor, Dr. Nimish N. Vachharajani. This research work was funded by Drugs for Neglected Diseases *Initiative*, Geneva, Switzerland and was supported by a grant from the Bill and Melinda Gates Foundation/USA, with complementary core funding from Department for International Development (DFID)/UK, Federal Ministry of Education and Research (BMBF) through KfW/Germany and Médecins Sans Frontières (Doctors without Borders) International.

## References

Chaturvedi, P.R. et al., 2001. Prediction of pharmacokinetic properties using experimental approaches during early drug discovery. Curr. Opin. Chem. Biol. 5, 452–460.

Davies, B., Morris, T., 1993. Physiological parameters in laboratory animals and humans. Pharm. Res. 10, 1093–1095.

Dogra, M. et al., 2011. Comparative bioactivation of the novel anti-tuberculosis agent PA-824 in Mycobacteria and a subcellular fraction of human liver. Br. J. Pharmacol. 162, 226–236.

Flockhart, D.A., 2007. Drug Interactions: Cytochrome P450 Drug Interaction Table. Indiana University School of Medicine. <http://medicine.iupui.edu/clinpharm/ddis/table.asp>.

Gupta, S. et al., 2013. Nitroimidazo-oxazole compound DNDi-VL-2098 as a candidate for oral treatment of Visceral Leishmaniasis. In: Proceeding of: 5th International symposium on Drug Development for Orphan-Neglected Diseases (CTDDR-2013), Abs. No. P-75, pp. 134.

Harisudhan, T. et al., 2011. Preclinical pharmacokinetics and prediction of human PK of DNDI-VL-2098, a potential oral treatment for visceral leishmaniasis. In: Poster presented at AAPS.

Mahmood, M., 2007. Application of allometric principles for the prediction of pharmacokinetics in human and veterinary drug development. Adv. Drug Deliv. Rev. 59, 1177–1192.

Mehmood, I., Balian, J.D., 1996. Interspecies scaling: predicting clearance of drugs in humans: three different approaches. Xenobiotica 26, 887–895.

Olliaro, P.L. et al., 2005. Treatment options for visceral leishmaniasis: a systematic review of clinical studies done in India, 1980–2004. Lancet. Infect. Dis 5, 763–774.

Rao, M. et al. 2011. In-vitro metabolism and disposition of DNDI-VL-2098, a potential treatment for visceral leishmaniasis. In: Poster Presented at AAPS.

Romero, G.A.S., Boelaert, M., 2010. Control of visceral leishmaniasis in Latin America — a systematic review. PLoS Neglected Tropical Diseases 4 (1), e584. http://dx.doi.org/10.1371/journal.pntd.0000584.

Sharma, V., McNeill, J.H., 2009. To scale or not to scale: the principles of dose extrapolation. Br. J. Pharmacol. 157, 907–921.

Sundar, S. et al., 2000. Failure of pentavalent antimony in visceral leishmaniasis in India: report from the center of the Indian epidemic center. Clin. Infect. Dis. 31 (4), 1104–1107.

Sundar, S. et al., 2012. Efficacy of miltefosine in the treatment of visceral leishmaniasis in India after a decade of use. Clin. Infect. Dis. 55 (4), 543–550.

Van Griensven, J. et al., 2010. Combination therapy for visceral leishmaniasis. Lancet. Infect. Dis 10, 184–194.

Veber, D.F. et al., 2002. Molecular properties that influence the oral bioavailability of drug candidates. J. Med. Chem. 45, 2615–2623.